

Article

Adaptive Synergetic Motion Control for Wearable Knee-Assistive System: A Rehabilitation of Disabled Patients

Shaymaa M. Mahdi ¹, Noor Q. Yousif ¹, Ahmed A. Oglah ¹, Musaab E. Sadiq ², Amjad J. Humaidi ^{1,*} and Ahmad Taher Azar ^{3,4}

¹ Department of Control and Systems Engineering, University of Technology-Iraq, Baghdad 10001, Iraq; shaymaa.m.mahdi@uotechnology.edu.iq (S.M.M.); 60165@uotechnology.edu.iq (N.Q.Y.); ahmed.a.oglah@uotechnology.edu.iq (A.A.O.)

² Ministry of Trade, General Company for Grain Processing, Baghdad 10001, Iraq; mesmsi50@gmail.com

³ College of Computer and Information Sciences, Prince Sultan University, Riyadh 11586, Saudi Arabia; aazar@psu.edu.sa

⁴ Faculty of Computers and Artificial Intelligence, Benha University, Benha 13518, Egypt; ahmad.azar@fci.bu.edu.eg or ahmad_t_azar@ieee.org

* Correspondence: amjad.j.humaidi@uotechnology.edu.iq

Abstract: In this study, synergetic-based adaptive control design is developed for trajectory tracking control of joint position in knee-rehabilitation system. This system is often utilized for rehabilitation of patients with lower-limb disabilities. However, this knee-assistive system is subject to uncertainties when applied to different persons undertaking exercises. This is due to the different masses and inertias of different persons. In order to cope with these uncertainties, an adaptive scheme has been proposed. In this study, an adaptive synergetic control scheme is established, and control laws are developed to ensure stable knee exoskeleton system subjected to uncertainties in parameters. Based on Lyapunov stability analysis, the developed adaptive synergetic laws are used to estimate the potential uncertainties in the coefficients of the knee-assistive system. These developed control laws guarantee the stability of the knee rehabilitation system controlled by the adaptive synergetic controller. In this study, particle swarm optimization (PSO) algorithm is introduced to tune the design parameters of adaptive and non-adaptive synergetic controllers, in order to optimize their tracking performances by minimizing an error-cost function. Numerical simulations are conducted to show the effectiveness of the proposed synergetic controllers for tracking control of the exoskeleton knee system. The results show that compared to classical synergetic controllers, the adaptive synergetic controller can guarantee the boundedness of the estimated parameters and hence avoid drifting, which in turn ensures the stability of the controlled system in the presence of parameter uncertainties.

Keywords: exoskeleton knee system; synergetic control; adaptive law; particle swarm optimization (PSO)



Citation: Mahdi, S.M.; Yousif, N.Q.; Oglah, A.A.; Sadiq, M.E.; Humaidi, A.J.; Azar, A.T. Adaptive Synergetic Motion Control for Wearable Knee-Assistive System: A Rehabilitation of Disabled Patients. *Actuators* **2022**, *11*, 176. <https://doi.org/10.3390/act11070176>

Academic Editor: Hicham Chaoui

Received: 3 May 2022

Accepted: 14 June 2022

Published: 22 June 2022

Publisher's Note: MDPI stays neutral with regard to jurisdictional claims in published maps and institutional affiliations.



Copyright: © 2022 by the authors. Licensee MDPI, Basel, Switzerland. This article is an open access article distributed under the terms and conditions of the Creative Commons Attribution (CC BY) license (<https://creativecommons.org/licenses/by/4.0/>).

1. Introduction

The World Health Organization (WHO) has reported that 15 million people worldwide have suffered strokes and 5 million have been left disabled for a long time. The main causes of acute and long-term disabilities are neurological injuries such as strokes, heart attacks and spinal cord injuries (SCIs) [1].

Mobility and autonomy can be lost in patients suffering from musculoskeletal lesions and neurological problems. This can lead to many physical symptoms such as muscle weakness, partial or complete loss of sensation, poor cognitive abilities, and decreased alertness. These in turn have an adverse effect on a patient's welfare. Medical reports have shown that a cure is possible for many such patients if they strictly follow programs of physical rehabilitation and therapy. Fruitful remedial results could be obtained if the

patients are enabled to perform certain tasks after undertaking long-term and repeated exercises [1,2].

During the repeated treatments, exercises are prescribed for disabled individuals and performed manually by the physicians supervising the treatment. This treatment is costly as it requires the involvement of physicians and movement-supervising doctors for each patient [2,3].

In order to mitigate the reliance on these time-consuming rehabilitation exercises, actuated bio-engineering exoskeletons have been used as alternatives. Due to the repetitive physical movements, these assisting devices can assist multiple patients simultaneously and hence alleviate therapists' workloads. In addition, these robot-assisted orthoses are capable of measuring, quantifying, and recording the treatment progress for each patient by employing special sensors, which are responsible for various measurements such as angular position, velocity, exerted torque, etc. The physicians can then analyze and interpret the reports so that the treatment can be modified accordingly. According to clinical trials and reports, these robotic exoskeleton systems have demonstrated high effectiveness and good efficacy [2,3].

One critical consideration while following such type of remedy and rehabilitation is that the exoskeleton-like robot must be customized to fit the dimension of human joint and its range of mobility. The assisting devices must be coupled to the patient's body in such a way that ergonomic motion has to be tolerated by the patient wearer. This critical point to be taken into account, especially regarding lower-limb orthoses, where these exoskeleton-like robots have the ability to retrieve when subjected to repetitive movements such that the patient's independence and autonomy can be eventually regained [2,3].

An exoskeleton knee-assisted robot is composed of two articulated links: one is attached and fixed to the human thigh and the other moves with the leg shank. The exoskeleton system uses a DC motor at the knee joint to actuate the assistive system with the torque required to assist the movement of the disabled knee smoothly and accurately. To achieve smooth and accurate movement, control theory is required. In addition, there is a crucial problem concerning the exact modeling and precise parameter acquisition for the exoskeleton knee-assistive system, especially if the system is used or worn by more than one person, with different physical attributes. Therefore, adaptive, robust, and accurate control schemes have become an inevitable demand, as the key points of this application. In view of this point, a literature review and a brief discussion address the relevant research devoted to motion control for exoskeleton lower-limb systems.

In [4], Rifaï et al. developed a model-reference adaptive control (MRAC) for controlling the motion of a shank-orthosis system in the presence of uncertainties in parameters. Assuming a bounded torque application such as exercises for persons, the input-to-state and asymptotic stabilities have been proved in the case of the exertion of non-muscular effort. In [5], Kashif et al. presented an adaptive control design for "Exoskeleton Intelligently Communicating and Sensitive to Intention (EICoSI)" based on the robust integral of sign error (RISE) methodology. The proof of asymptotic stability in semi-global sense was shown for a linked exoskeleton-human system. Compared to conventional RISE control, the adaptive RISE control showed less tracking error and higher robustness. In [6], Mithaq et al. presented position-to-force motion control design of knee-joint in active lower-limb prostheses. A hybrid controller is synthesized based on a PID controller in conjunction with ANFIS (adaptive neuro-fuzzy inference system). Compared to individual PID controllers and ANFIS controllers, the ANFIS-PID control showed better dynamic performance. In [7], Ding et al. proposed proxy-based adaptive sliding mode control (SMC) to achieve trajectory tracking of a shank-orthosis system in the presence of parametric uncertainty. Compared to traditional and adaptive PID controllers and proxy-based SMC, the proxy-based adaptive SMC showed better performance in terms of tracking accuracy and robustness characteristics. In [8], Mefoued et al. presented the design of high-order sliding mode controller to perform flexion-extension movements of the knee joint in order to assist the rehabilitation of persons suffering problems with lower-limb mobility. Com-

pared to classical PID controller, the sliding mode controller exhibited better performance in terms of tracking error, robustness characteristics, stability, and finite-time convergence of error trajectories. In [9], Zhao, W. and Song, A. proposed a novel proxy-based sliding mode controller (PSMC) to improve trajectory tracking accuracy of an exoskeleton knee actuated by pneumatic artificial muscle (PAM). Compared to conventional controllers, the PSMC showed better tracking performance in terms of accuracy and robustness. In [10], Ajayi et al. presented bounded control scheme to assist persons suffering from disorders in their lower limbs. In order to fulfill the requirement of bounded human torque, high-gain observer (HGO) has been applied to estimate the joint torques. The developed control law resulted in good tracking performance of the controlled system subjected to a physiotherapeutic trajectory. In [11], Sierra et al. developed an actuating configuration using a harmonic-drive DC motor together with PAM to actuate the lower-limb exoskeleton. This actuating technology gives a high power/weight ratio and better position accuracy, and hence improves the functional performance of human lower limbs. The PID controllers are utilized for motion control of the limbs. In [12], Lee et al. proposed a sliding mode control design for a polycentric knee exoskeleton (PKE) system to cope with system uncertainty and nonlinearity. To solve the low-load capacity problem of actuator, the knee system is powered by an electro-hydraulic actuator (EHA). The proposed controller showed good tracking performance. In [13], Rifaï et al. designed an L1 adaptive controller for trajectory tracking control of knee joint motion for an exoskeleton system of type-EICoSI. The delay problem, caused by a filter in control scheme, can be solved by introducing nonlinear proportional control to give an augmented L1 adaptive controller. Compared to the classical L1 adaptive controller, the augmented version showed better robustness and dynamic performance. In [14], Mefoued and Belkhiat designed robust controller for motion control of knee-assistive system to enable limited-knee movement of disabled people. The control scheme incorporated parameter identification process for the lower-limb exoskeleton system. A sliding mode observer (SMO) was used to estimate the velocity and position of the knee joint. The designed controller showed good performance in terms of trajectory tracking errors and robustness characteristics under variations in system parameters. In [15], C. Chen could improve the tracking performance of lower-limb exoskeleton system by proposing control design based on active disturbance rejection control (ADRC) and fast terminal SMC. The lumped disturbance is estimated utilizing extended state observer (ESO). The proposed controller showed faster response and better tracking precision as compared to a PID controller. In [16], J. Wang investigated the control design for a PAM-actuated lower-extremity exoskeleton (LEE) system using output sliding mode control (SMC) based on a finite-time observer. This study applied a finite-time ESO to estimate the lumped disturbances and unmeasurable velocities. The proposed observer-based SMC showed good tracking performance with high precision. In [17], Chevalier A. et al. presented control design based on fractional-order proportional-integral (FOPI) control for shank-motion control around the knee joint. This study utilized integer-order transfer functions with finite dimensions to synthesize and approximate the FOPI. Compared to an integer-order PI controller, the POPI controller showed higher disturbance rejection capability and better robustness characteristics.

In [18], S. Kaur et al. applied the control design based on fractional-order PID (FOPID) control for trajectory tracking control of knee joint angle. The study adopted traditional trial-and-error procedure and internal mode control (IMC) for tuning the controller's design parameters. The proposed controller demonstrated good robustness characteristics against variations in system parameters. In [19], S. Mefoued et al. presented high-precision motion of a knee-joint orthosis based on a second-order sliding mode control (SMC) design under nonparametric and parametric uncertainties. The orthosis is intended to assist people with reduced mobility to achieve restored knee-joint movements. Compared to classical control, the proposed controller showed satisfactory performance and efficacy in terms of tracking errors and robustness. In [20], S. Mefoued proposed an intelligent adaptive controller based on an MLPNN (multi-layer perceptron neural network) for controlling flexion and extension

motions of the knee. Knowledge of the dynamic model is not required in the control design, and the controller is capable of dealing with all uncertainties in the system parameters, modeling, and coupling. The proposed adaptive MLPNN-based controller showed better efficacy and tracking performance than a PID controller. In [21], T. K. Wang et al. addressed the nonlinear and time-varying coupling between the human thigh and a prosthetic limb by introducing adaptive control for knee-joint motion. The proposed adaptive controller could improve the appearance of the gait pattern, adapt to walking speed, and compensate for variations in hip movement. In [22], Zhang Y. et al. adopted a model-free adaptive control strategy for motion control of the human–exoskeleton assistive system at the knee joint level. Uncertainties due to the modeling complexity of assistive systems were considered, and the controller performed its task based on input–output data acquisition for the knee-joint angle. In [23], Guan W. et al. have proposed iterative learning control algorithm for motion control of lower-limb exoskeleton system devoted for human knee joint and hip. The control algorithm has been designed based on musculoskeletal model and the parameter identification has been conducted for different subjects. The accuracy of gait tracking of exoskeleton system is considerably enhanced and the follow-up performance has been greatly improved. In [24], Aljuboury et al. presented the design of three control schemes based on model reference adaptive control (MRAC) for an exoskeleton knee assistance system. This study showed that the observer-based MRAC outperformed the classical MRAC and adaptive MRAC in terms of robustness characteristics and tracking accuracy. In [25], Aole et al. introduced improved active disturbance-rejection control (I-ADRC) for trajectory tracking of a 2-DOF lower limb robotic rehabilitation exoskeleton (LLRRE). The proposed controller showed better trajectory tracking, better ability to reject disturbances and noise, and high robustness with respect to parameter variations. In [26], Zhan Li et al. proposed a novel control scheme for tracking control of a knee exoskeleton system subjected to time-varying viscous and inertial coefficients due to disturbances in interaction torque. The proposed approach showed exponentially zero convergence for the tracking joint-angle error, bounded tracking error under interaction torque, and better efficiency in terms of tracking performance as compared to other control techniques. In [27], M. K. Shepherd and E. J. Rouse introduced a novel series elastic actuator to produce the required torques and speeds for sit-to-stand assistance. The proposed actuating technology reduced the output impedance and improved the torque control to a large extent. A high-level sit-to-stand controller was implemented for a unilateral orthosis based on the proposed actuator, to assist three able-bodied subjects. In [28], Lyu M. et al. developed a knee exoskeleton device controlled by electromyography (EMG) to assist rehabilitation of stroke patients in their homes. The patients were encouraged to be involved in a new designed game during the training process, to enhance the rehabilitation performance. The test demonstrated that the EMG signals could control the exoskeleton, which assists the patients in playing the game.

Based on above literature, it has been shown that the use of sliding mode control with its different versions could give efficient and robust control characteristics, especially for this uncertain assistive system. However, one critical drawback which has been reported for SMC is the inevitable appearance of chattering behavior in the control signal. A great deal of research has been devoted to solve this problem, and the effect has been reduced but not removed. This was the motivation to turn towards synergetic control theory, which has the same control features as SMC but avoids chattering.

The Synergetic control (SC) methodology is based on state-space theory. Recently, this control methodology has been applied to highly connected and complex nonlinear systems. Controller designed based on SC could drive the system's state variables in such a way as to follow an invariant manifold, which is designed to satisfy the required control specifications in the presence of nonparametric and parametric uncertainties [29–31]. A design based on synergetic control for nonlinear systems has the following advantages:

- Establishing an extended system of differential equations (DEs). These DEs reflect various operations such as coordinate observation, optimization, disturbance suppression, etc.

- Reducing the extra degrees of freedom (DOF) of extended system w.r.t final manifold by synthesizing an “external” control. The motion can be described by the “internal” dynamics equations of the system.
- Developing the “internal” controls, which are responsible for establishing links between the “internal” coordinates of the system such as to satisfy the control objective.

The synergetic controller could guide the system’s trajectories from initial states to their equilibrium points onto a manifold. It has been shown that the design parameters, emerging in development of controllers, have a direct effect on their performances. Often, these design parameters are chosen according to conventional trial-and-error method. One drawback of this procedure is that it does not find the optimal solutions in terms of these parameters and the cost index. Therefore, a modern optimization algorithm is employed to optimize design parameters for further improving the controlled system’s dynamic performance [32,33]. The present study uses particle swarm optimization (PSO) to fine-tuning the design parameters. Kennedy first introduced this optimization technique in 1995. The technique is inspired by the behavior of organisms [34,35]. This fine tuner is characterized by rapid convergence rate, high computational efficiency, and ability to find both global and local solutions. The contribution of this study can be highlighted by the following points:

- Design of a synergetic control law for a knee-assistive system based on the synergetic control methodology.
- Design of adaptive laws for an adaptive synergetic controller for a knee-assistive system based on Lyapunov stability analysis, to deal with uncertainties in the system.
- Conduction stability analysis to ensure a stable system and to guarantee the ultimate boundedness of estimated gains.
- Design of an optimization algorithm to tune the design parameters of both classical and adaptive synergetic controllers.

2. Modeling of Exoskeleton Knee-Assistive System

An exoskeleton-aided knee system is composed of two links, as shown in Figure 1. One link is stationary and is attached to thigh, while the other link moves over an angular range and is attached to the shin. The second link is actuated and rotated by a DC motor fixed at the knee joint. In the case of a disabled knee, the motor is responsible for generating the required torque to accurately rotate the leg into the desired position. As indicated in Figure 1, the exoskeleton system was configured to operate in the range $[0^\circ - 90^\circ]$. Full extension of the leg is indicated by 0° , while 90° represents the resting position of the leg [36].

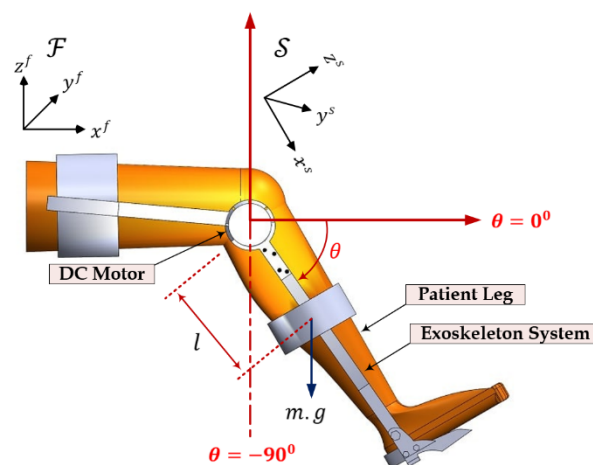


Figure 1. The geometric representation of knee-exoskeleton system dynamic.

According to Figure 1, two frames can be identified: the global frame \mathcal{F} and the local frame \mathcal{S} . The global frame is an earth-centered fixed frame defined by $(\vec{x}^f, \vec{y}^f, \vec{z}^f)$, and the local frame (exoskeleton frame) is defined by $(\vec{x}^s, \vec{y}^s, \vec{z}^s)$. It rotates at the same joint angle θ , and the axes of the frames \vec{y}^f and \vec{y}^s coincide during the orientation of the local frame. It is clear that one degree of freedom (DOF) is observed for knee-joint movements. Therefore, the time derivative of the knee joint angle θ represents the angular velocity $\dot{\theta}$ of the joint.

The dynamic models of the human leg and exoskeleton are developed simultaneously using the Lagrangian method. Lagrangian-based dynamic modeling of the coupled system (human leg and exoskeleton device) is initiated with the expression:

$$\ell_i = E_{ki} - E_{gi} \tag{1}$$

where $i \in (1,2)$ denotes the components of the human leg and exoskeleton, and E_{gi} and E_{ki} represent the gravitational and kinetic energies of the system elements, respectively.

$$E_{ki} = \frac{1}{2} J_i \dot{\theta}^2 \tag{2}$$

where J_i represent the inertias of the system components (human leg and exoskeleton), and

$$E_{gi} = m_i \cdot g \cdot l_i \cdot (1 - \sin\theta) \tag{3}$$

where m_i , g , and l_i represent the mass of the leg and exoskeleton system, the acceleration due to gravity, and the distance between the center of gravity and the knee joint, respectively.

Based on the Euler–Lagrange differential equation of ℓ_i , the dynamic model of the combined system components can be obtained:

$$J_i \ddot{\theta} = m_i \cdot g \cdot l_i \cdot \cos\theta - \tau_{exti} \tag{4}$$

where τ_{exti} represents the total externally applied torque, which is composed of two components given by

$$\tau_{exti} = \tau_{fi} + \tau_i \tag{5}$$

where τ_i is the control torque generated by the DC motor and τ_{fi} is the friction torque given by

$$\tau_{fi} = -f_{si} \operatorname{sgn}\dot{\theta} - f_{vi} \dot{\theta} \tag{6}$$

where f_{vi} and f_{si} denote the viscous friction and solid friction coefficients, respectively. One can express the dynamic model of the coupled exoskeleton–human leg system as follows:

$$J \ddot{\theta} = -\tau_g \cos\theta - f_s \operatorname{sgn}\dot{\theta} - f_v \dot{\theta} + \tau_h + \tau \tag{7}$$

where $f_s = \sum_{i=1}^2 f_{si}$, $f_v = \sum_{i=1}^2 f_{vi}$, $\tau_g = \sum_{i=1}^2 \tau_{gi}$, and $J = \sum_{i=1}^2 J_i$. The angular position, velocity, and acceleration of the coupled system are represented by the variables θ , $\dot{\theta}$, and $\ddot{\theta}$, respectively. The parameters J , τ_g , τ , and τ_h represent the inertia of the coupled system (exoskeleton–human leg) and the gravity torque, the control torque, and the load torque due to the coupled system, respectively.

The state variable of Equation (7) can be established for control purposes by assigning the states x_1 and x_2 to the variables θ and $\dot{\theta}$, respectively. This gives

$$\begin{aligned} \dot{x}_1 &= x_2 \\ \dot{x}_2 &= \frac{1}{J} [\tau - f_v x_2 - f_s \operatorname{sign}(x_2) + \tau_g \cos(x_1)] \end{aligned} \tag{8}$$

3. Classical and Adaptive Control Design for Knee-Assistive System

In this part, tracking control design based on two control approaches are developed for the angular position of knee-assistive system. The first step of control design is based on non-adaptive synergetic control method, while the next control design is conducted based on adaptive synergetic control approach when the system is subjected disturbance or parameter uncertainties.

3.1. Synergetic Control Design for Knee-Assistive System

The design is initiated by defining the error e to be the difference between the actual state ($x_1 = \theta$) and desired trajectory ($x_{1d} = \theta_d$)

$$e = x_1 - x_{1d} \quad (9)$$

Taking the first and second derivatives of error equation to have

$$\dot{e} = \dot{x}_1 - \dot{x}_{1d} = x_2 - \dot{x}_{1d} \quad (10)$$

$$\ddot{e} = \dot{x}_2 - \ddot{x}_{1d} \quad (11)$$

Let $\psi(x)$ represents the macro variable, which is defined by

$$\psi(e) = c \cdot e + \dot{e} \quad (12)$$

Taking the first time derivative of Equation (12), we have

$$\dot{\psi}(e) = c \cdot \dot{e} + \ddot{e} \quad (13)$$

where c is a scalar design parameter.

The dynamic evolution of macro-variables towards the manifolds is described by [20]:

$$T \cdot \dot{\psi}(e) + \psi(e) = 0, T > 0 \quad (14)$$

where T denotes the convergence rate of system trajectory. This dynamic is dependent, in order to ensure that the trajectories of all state variables achieve the desired manifold and stay on it for future time [21].

Using Equations (12)–(14), one can obtain

$$T(c \dot{e} + \ddot{e}) + \psi(e) = 0 \quad (15)$$

or

$$T\dot{x}_2 - T\ddot{x}_{1d} + Tc \dot{e} + \psi(e) = 0 \quad (16)$$

Substituting Equation (8) into Equation (16), we have

$$\frac{T}{J} [u - f_v x_2 - f_s \text{sign}(x_2) + \tau_g \cos(x_1)] - T\ddot{x}_{1d} + Tc \dot{e} + \psi(e) = 0 \quad (17)$$

where u represents the control signal. In order to satisfy $T \dot{\psi}(e) + \psi(e) = 0$, the control law can be developed based on Equation (17) as follows:

$$u = [f_v x_2 + f_s \text{sign}(x_2) - \tau_g \cos(x_1)] + J \ddot{x}_{1d} - J c \dot{e} - J \psi(e)/T \quad (18)$$

3.2. Design of ABSMC for Knee Exoskeleton System

This part of control design addresses and solves the problem of uncertainty that occurs in physical parameters of the knee-exoskeleton assistive system. The adaptive control algorithm is responsible for suppressing undesired effects of disturbances, which in turn have an adverse effect on the tracking performance. This study developed adaptive scheme

based on synergetic control concept to establish the necessary adaptive laws that can estimate and reduce the effect of uncertainty in system parameters such that the stability of controlled rehabilitation system can be ensured.

The uncertainty will be discussed for three coefficients: the viscous damping coefficient of the knee and the exoskeleton device f_v , the solid friction coefficient of the knee and the exoskeleton f_s , and the gravitational torque coefficient τ_g .

$$\hat{f}_v = f_v - \tilde{f}_v \tag{19}$$

$$\hat{f}_s = f_s - \tilde{f}_s \tag{20}$$

$$\hat{\tau}_g = \tau_g - \tilde{\tau}_g \tag{21}$$

where \hat{f}_v represents the estimated value of the f_v coefficient, \hat{f}_s is the estimated value of the f_s coefficient, and $\hat{\tau}_g$ represents the estimated value of the τ_g coefficient, while \tilde{f}_v , \tilde{f}_s , and $\tilde{\tau}_g$ are the variations in the above coefficients, respectively.

The candidate LF can be defined as

$$V = \frac{1}{2} \psi(e)^2 + \frac{1}{2} \gamma_1^{-1} \tilde{f}_v^2 + \frac{1}{2} \gamma_2^{-1} \tilde{f}_s^2 + \frac{1}{2} \gamma_3^{-1} \tilde{\tau}_g^2 \tag{22}$$

where γ_1 , γ_2 , and γ_3 denote the adaptation gains of control laws. Taking the time derivative of Equation (22), we have

$$\dot{V} = \psi(e) \dot{\psi}(e) - \gamma_1^{-1} \tilde{f}_v \dot{\tilde{f}}_v - \gamma_2^{-1} \tilde{f}_s \dot{\tilde{f}}_s - \gamma_3^{-1} \tilde{\tau}_g \dot{\tilde{\tau}}_g \tag{23}$$

Based on Equations (13) and (23), one can obtain

$$\dot{V} = \psi(e) (c \dot{e} + \ddot{e}) - \gamma_1^{-1} \tilde{f}_v \dot{\tilde{f}}_v - \gamma_2^{-1} \tilde{f}_s \dot{\tilde{f}}_s - \gamma_3^{-1} \tilde{\tau}_g \dot{\tilde{\tau}}_g \tag{24}$$

Substituting Equation (11) in Equation (24), we have

$$\dot{V} = \psi(e) (c \dot{e} + \dot{x}_2 - \ddot{x}_{1d}) - \gamma_1^{-1} \tilde{f}_v \dot{\tilde{f}}_v - \gamma_2^{-1} \tilde{f}_s \dot{\tilde{f}}_s - \gamma_3^{-1} \tilde{\tau}_g \dot{\tilde{\tau}}_g \tag{25}$$

Utilizing Equation (8), one can obtain

$$\dot{V} = \psi(e) \left(c \dot{e} + \frac{1}{J} [u - f_v x_2 - f_s \text{sign}(x_2) + \tau_g \cos(x_1)] - \ddot{x}_{1d} \right) - \gamma_1^{-1} \tilde{f}_v \dot{\tilde{f}}_v - \gamma_2^{-1} \tilde{f}_s \dot{\tilde{f}}_s - \gamma_3^{-1} \tilde{\tau}_g \dot{\tilde{\tau}}_g \tag{26}$$

In cases of uncertain measurements, the estimated values of f_v , f_s , and τ_g are fed to the control law instead of the actual measurements,

$$u = [\hat{f}_v x_2 + \hat{f}_s \text{sign}(x_2) - \hat{\tau}_g \cos(x_1)] + J \ddot{x}_{1d} - J c \dot{e} - J \psi(e)/T \tag{27}$$

Using the control law of Equation (27), one can obtain

$$\dot{V} = -\psi^2(e)/T + \psi(e) \left(\frac{1}{J} \left[(\hat{f}_v x_2 + \hat{f}_s \text{sign}(x_2) - \hat{\tau}_g \cos(x_1)) - f_v x_2 - f_s \text{sign}(x_2) + \tau_g \cos(x_1) \right] \right) - \gamma_1^{-1} \tilde{f}_v \dot{\tilde{f}}_v - \gamma_2^{-1} \tilde{f}_s \dot{\tilde{f}}_s - \gamma_3^{-1} \tilde{\tau}_g \dot{\tilde{\tau}}_g \tag{28}$$

Equation (28) can be rewritten as

$$\dot{V} = -\psi^2(e)/T + \frac{\psi(e)}{J} \left[(\hat{f}_v - f_v) x_2 + (\hat{f}_s - f_s) \text{sign}(x_2) - (\hat{\tau}_g - \tau_g) \cos(x_1) \right] - \gamma_1^{-1} \tilde{f}_v \dot{\tilde{f}}_v - \gamma_2^{-1} \tilde{f}_s \dot{\tilde{f}}_s - \gamma_3^{-1} \tilde{\tau}_g \dot{\tilde{\tau}}_g \tag{29}$$

Using Equations (19)–(21), we have

$$\dot{V} = -\psi^2(e)/T + \frac{\psi(e)}{J} \left[-\tilde{f}_v x_2 - \tilde{f}_s \text{sign}(x_2) + \tilde{\tau}_g \cos(x_1) \right] - \gamma_1^{-1} \tilde{f}_v \dot{\hat{f}}_v - \gamma_2^{-1} \tilde{f}_s \dot{\hat{f}}_s - \gamma_3^{-1} \tilde{\tau}_g \dot{\hat{\tau}}_g \quad (30)$$

or,

$$\dot{V} = -\psi^2(e)/T + \tilde{f}_v \left(-\frac{\psi(e)}{J} x_2 - \gamma_1^{-1} \dot{\hat{f}}_v \right) + \tilde{f}_s \left(-\frac{\psi(e)}{J} \text{sign}(x_2) - \gamma_2^{-1} \dot{\hat{f}}_s \right) + \tilde{\tau}_g \left(\frac{\psi(e)}{J} \cos(x_1) - \gamma_3^{-1} \dot{\hat{\tau}}_g \right) \quad (31)$$

In order to ensure negative definiteness of the \dot{V} function, the last terms must be set to zero, leading to the following adaptive laws:

$$\dot{\hat{f}}_v = -\gamma_1 \frac{\psi(e)}{J} x_2 \quad (32)$$

$$\dot{\hat{f}}_s = -\gamma_2 \frac{\psi(e)}{J} \text{sign}(x_2) \quad (33)$$

$$\dot{\hat{\tau}}_g = \gamma_3 \frac{\psi(e)}{J} \cos(x_1) \quad (34)$$

Since the time derivative of LF is negative definite ($\dot{V} < 0$), the proposed adaptive synergetic control scheme can ensure the asymptotic stability of the controlled system even with presence of uncertainties in the system parameters (f_v , f_s , and τ_g) of exoskeleton system.

Theorem 1. For the system described by Equation (8) that is subjected to uncertainties in the parameters f_v , f_s , and τ_g , the developed adaptive laws given by Equations (32)–(34) will guarantee the stability of the system controlled by the adaptive synergetic controller and also ensure the boundedness of estimated gains.

The critical limitation of this adaptive synergetic controller specifically for this application is that the inertia has not been accounted for. This is due to the presence of the moment of inertia in the denominator when developing the adaptive laws for the stability analysis. However, this problem can be solved by including an observer to estimate the uncertain inertia, though this is out of the scope of this study. The realization of adaptive synergetic control for exoskeleton assistive devices for knee rehabilitation is illustrated in Figure 2. The adaptive controller consists of two essential elements: the control law and the adaptive laws. The adaptive laws are responsible for estimating the uncertainties in the parameters f_v , f_s , and τ_g . These estimates are fed to the control law to generate the control signal necessary to actuate the DC motor of the exoskeleton device.

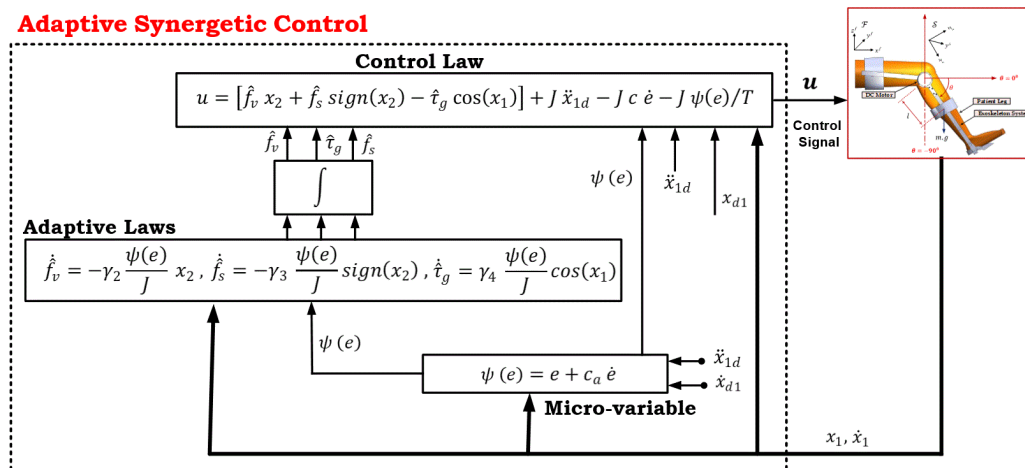


Figure 2. The realization of adaptive synergetic control for exoskeleton assistive devices for knee rehabilitation.

4. Results and Discussion

In this section, the effectiveness is verified for the classical and adaptive synergetic controllers, and a comparison study is conducted to show their performances in the presence of uncertainties. In this study, the parameters of the dynamic system were acquired from an estimation process, which was conducted as an experimental test on a healthy 33-year-old person, standing 1.73 m tall and weighing 75 kg. According to [14] and Table 1, the test was performed when the person was in a sitting position and wearing a lower-limb exoskeleton device.

Table 1. The identified parameters of exoskeleton system with sitting patient [14].

Coefficient Description	Value
Moment of inertia of leg-exoskeleton system J	0.348 kg·m ²
Viscosity damping coefficient of the knee and the exoskeleton f_v	0.872 N·m·s/rad
Solid friction coefficient of the knee and the exoskeleton f_s	0.998 N·m
Gravitation torque of the system τ_g	3.445 N·m

In this study, the PSO algorithm was chosen as a modern optimizer for optimal tuning of design parameters for the proposed controllers [32,33]. Optimization is required to further enhance the dynamic performance of knee-assistive controlled systems. For the classical synergetic control, the PSO technique was used to tune the design parameters C and T , while for the adaptive synergetic control, the tuned parameters were C , T , γ_1 , γ_2 , and γ_3 . These design parameters were tuned to minimize a cost function defined by root mean square of error (RMSE). The optimization process leads to optimal design parameters and hence to optimal controlled systems. Table 2 lists the optimal and non-optimal values of the design parameters for both conventional synergetic control (CSC) and adaptive synergetic control (ASC). The non-optimal settings of the parameters were based on a trial-and-error procedure.

Table 2. Non-Optimal and Optimal settings of ASC and CSC parameters.

Controller	Design Parameters	Setting Type of Design Parameters	
		PSO Algorithm	Trial-and-Error Technique
CSC	C	66.999	43.00
	T	0.000152	0.0322
ASC	C	34.910	50.00
	T	0.00092	0.0322
	γ_1	1.034	0.523
	γ_2	6.124	3.012
	γ_3	2.037	4.981

The envelope of the cost function over the algorithm iteration for the CSC-based knee-assistive system based on the PSO algorithm is illustrated in Figure 3. Figure 4 shows the trace for the cost function for the ASC-based knee-assistive system. It is clear from the figures that the tuner based on the PSO algorithm could effectively reduce the cost function with respect to iteration to reach optimal performance of controlled system.

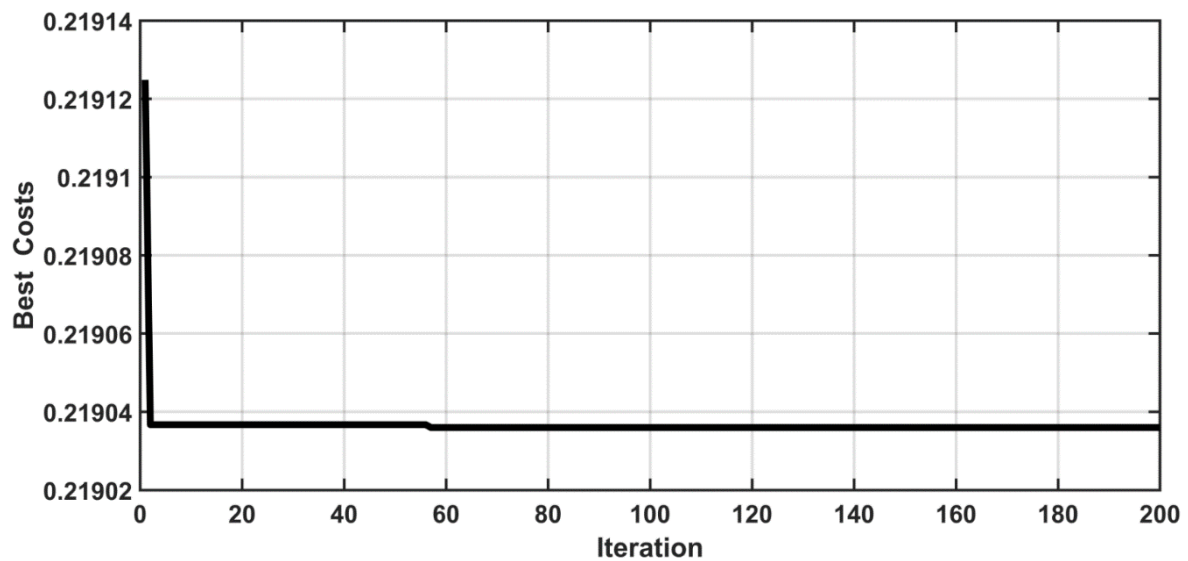


Figure 3. The cost-function behavior of CSC-controlled system based on PSO.

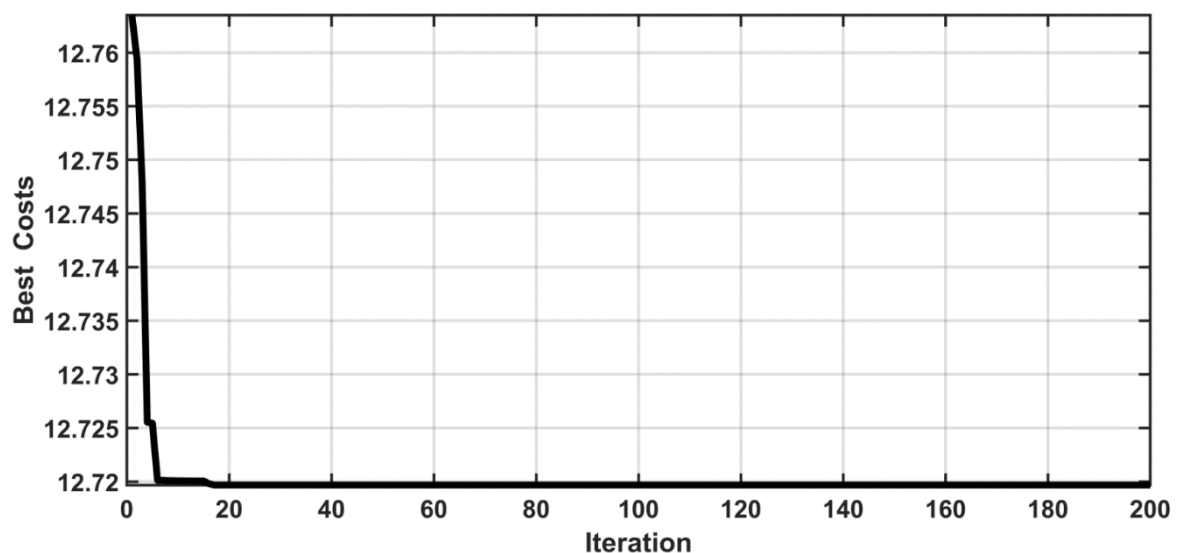


Figure 4. The cost-function behavior of ASC-controlled system using PSO algorithm.

Figure 5 shows the behavior of the knee angular positions around the mean angle of 40° , based on both optimal and conventional synergetic control. Based on Figure 5, the tracking errors can be extracted. These are illustrated in Figure 6. It is evident that the PSO algorithm improves transient characteristics more effectively than the trial-and-error procedure. The velocity at various angular positions is shown in Figure 7. A high value of velocity is shown at the initial condition due to the high slope at the simulation start-up moment.

In the next scenario, the responses of joint angular positions are shown in Figure 8 for both optimal and non-optimal adaptive synergetic control. The tracking error behaviors for both adaptive versions are shown in Figure 9. The figures show that the adaptive synergetic controller gives good tracking performance in both versions.

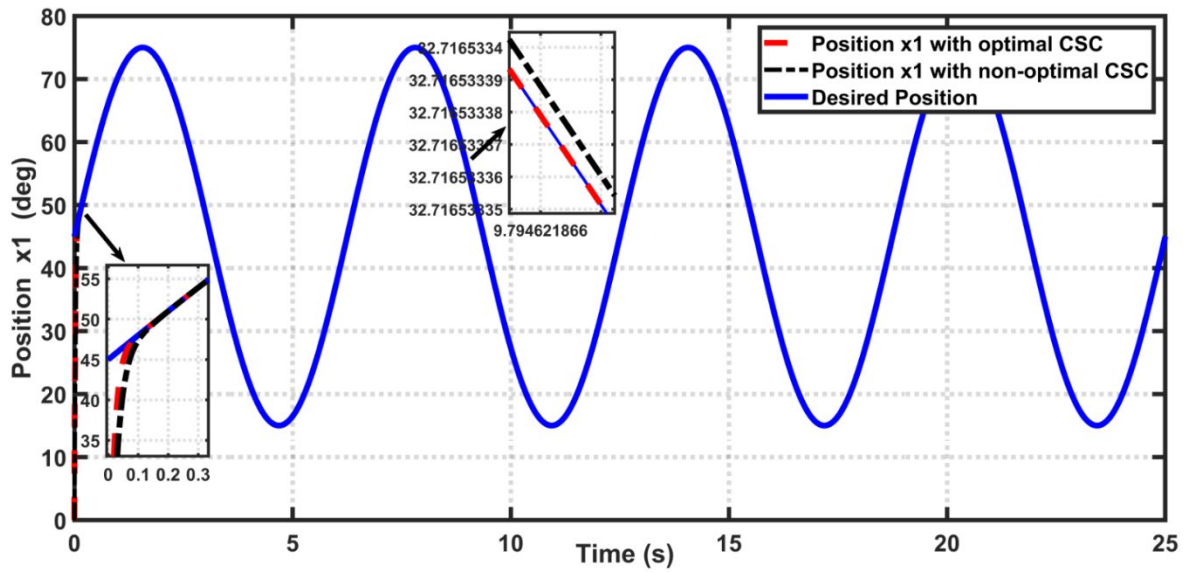


Figure 5. The transient behavior of knee angular position based on non-optimal and optimal synergetic control.

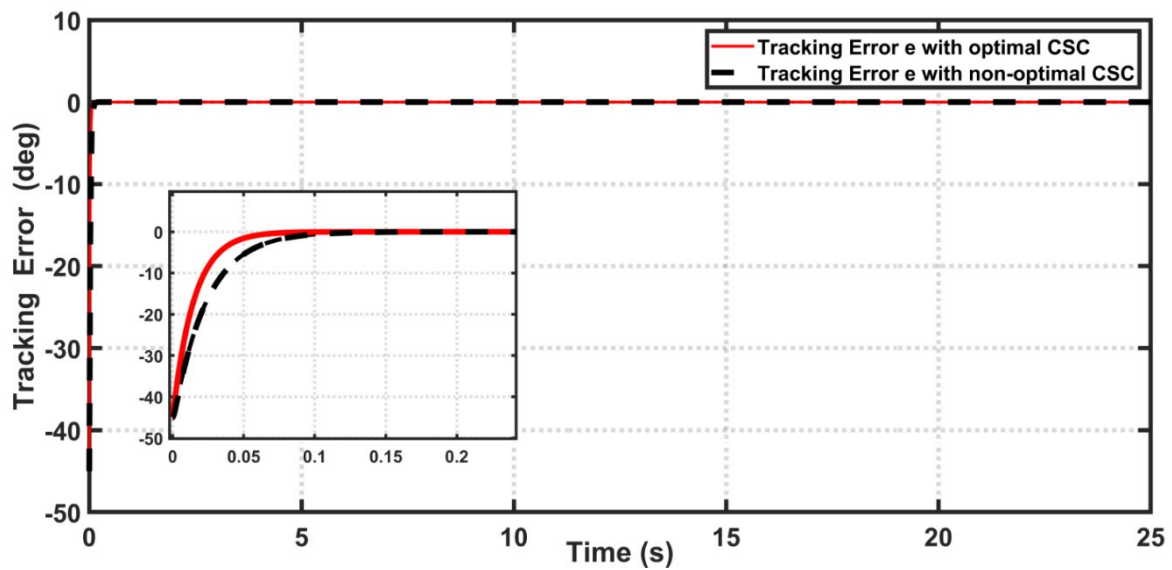


Figure 6. Behaviors of tracking errors for both non-optimal and optimal synergetic control.

The angular position velocities based on both versions of adaptive synergetic control are shown in Figure 10. Figure 11 shows the control signals generated by both adaptive synergetic controller schemes.

Figures 12–14 show the behaviors of the actual and estimated coefficients f_s , f_v , and τ_g resulting from the adaptive laws given by Equations (32)–(34), respectively. It is evident that due to the presence of uncertainty, the coincidence of both actual and estimated values may not be achieved. However, the boundedness of these estimated gains is necessary and sufficient to avoid the drift of these gains and hence to avoid instability problems.

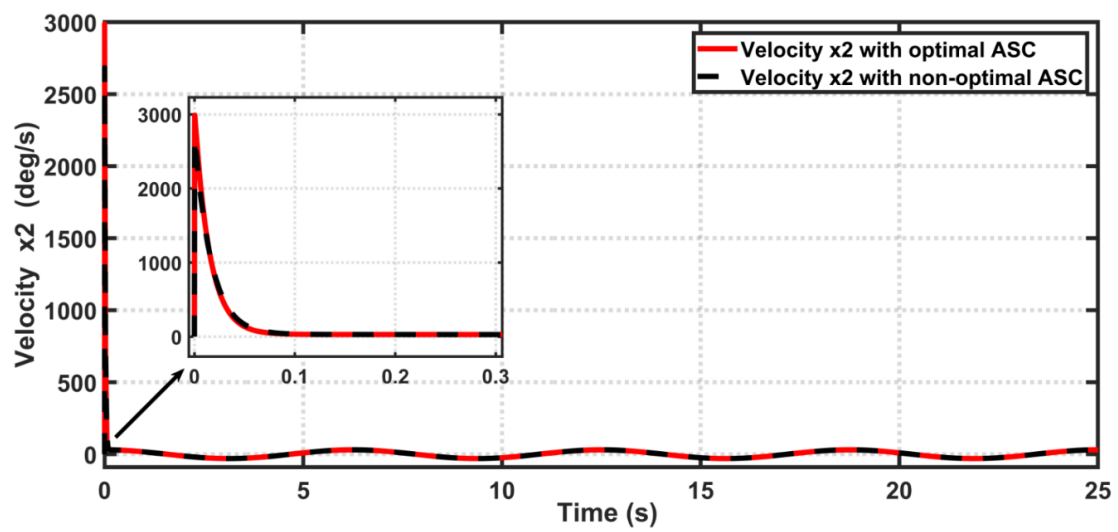


Figure 7. The velocity responses of joint angular positions.

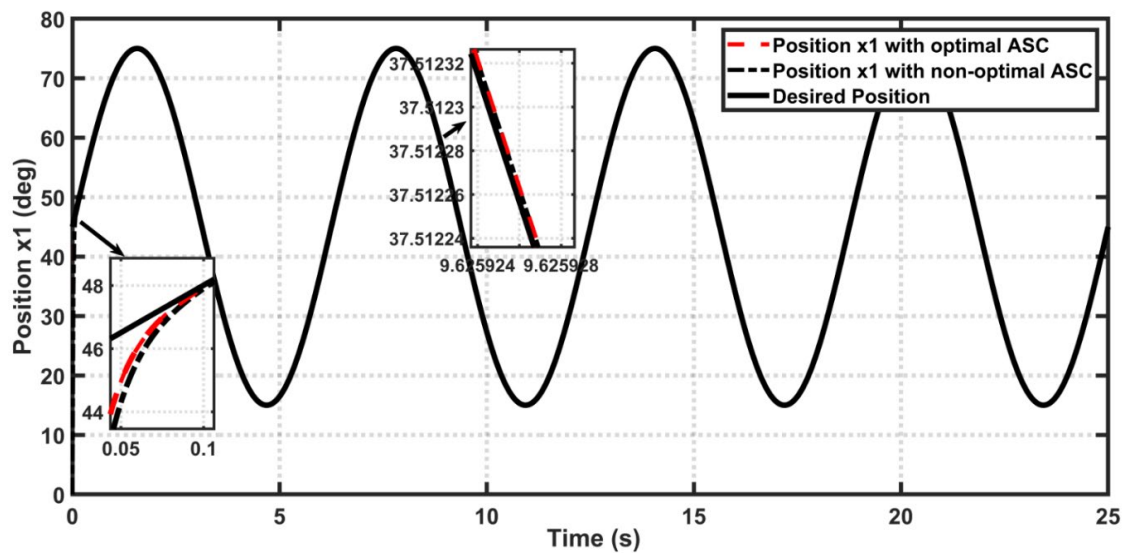


Figure 8. The behaviours of knee angular positions based on non-optimal and optimal ASC.

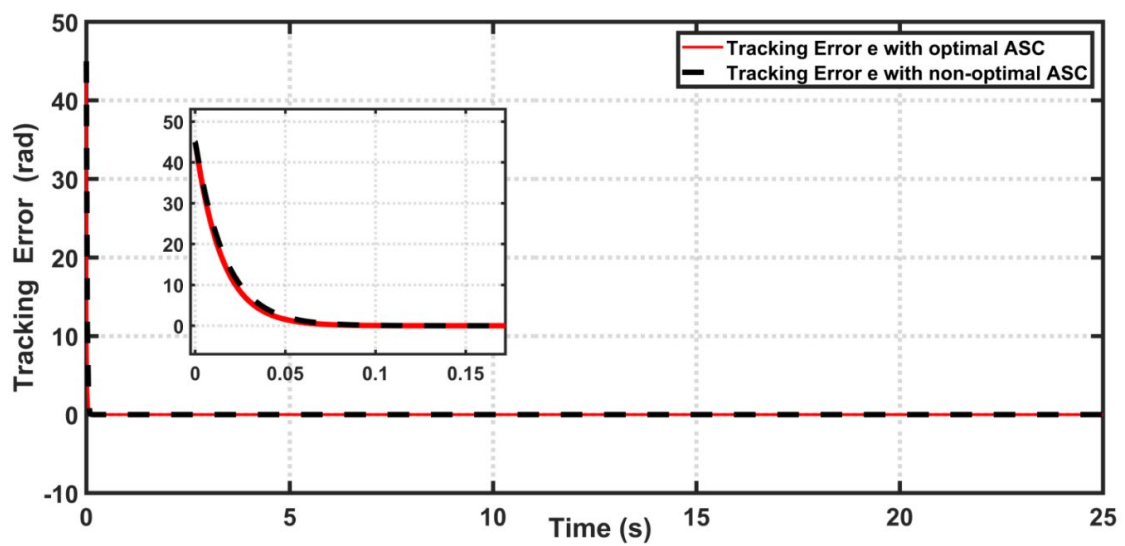


Figure 9. The responses of tracking errors based on non-optimal and optimal ASC.

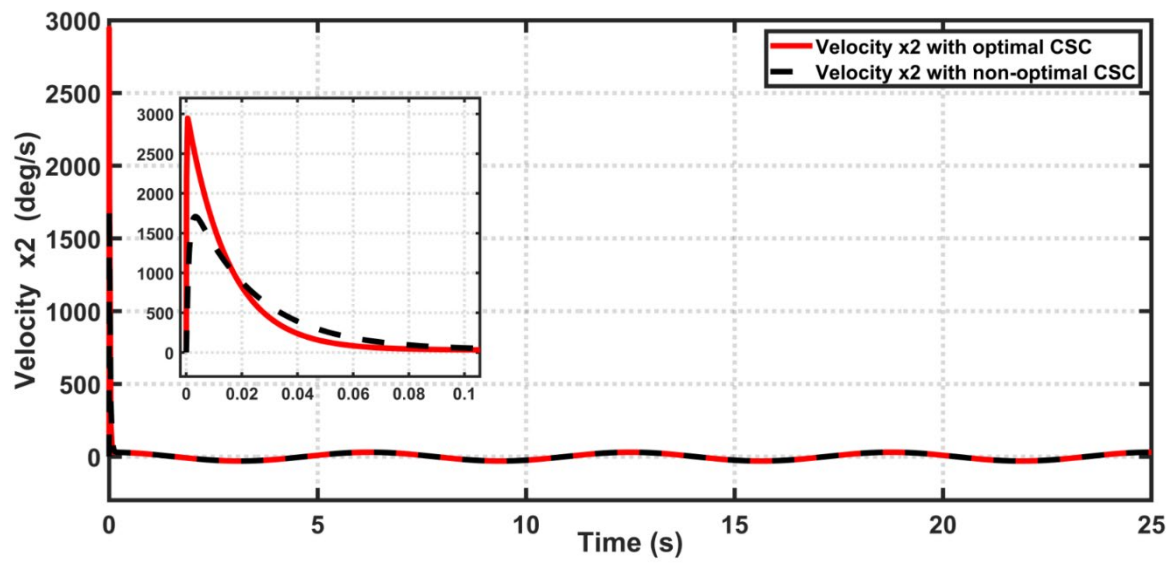


Figure 10. The velocity responses for optimal and non-optimal ASCs.

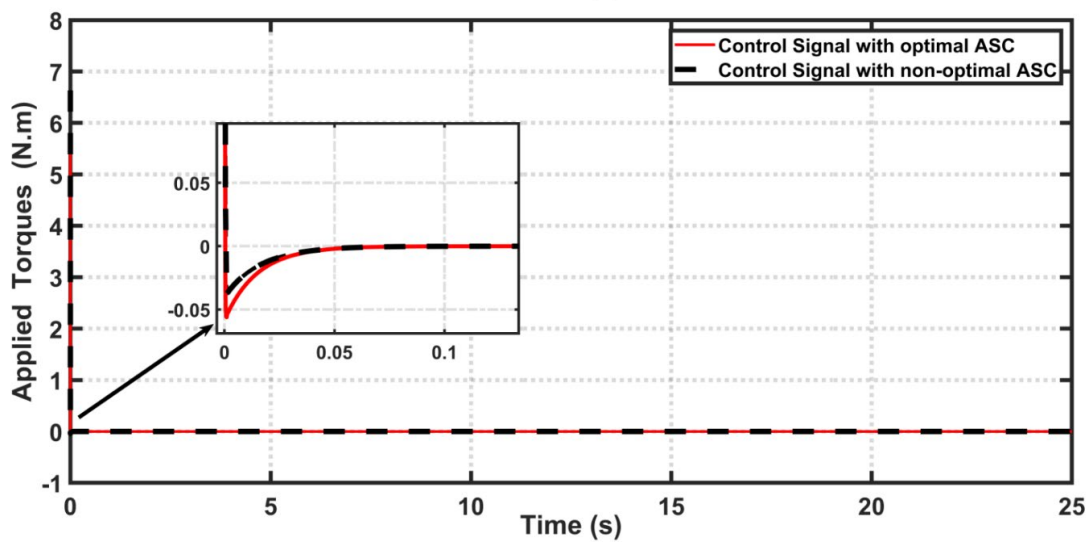
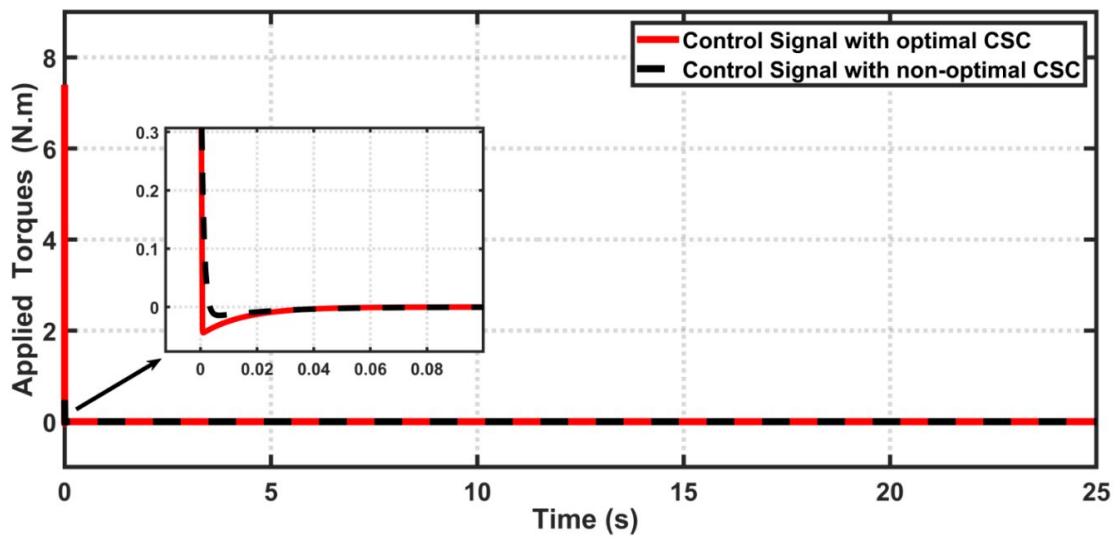


Figure 11. Control signals generated by optimal and non-optimal CSC and ASC.

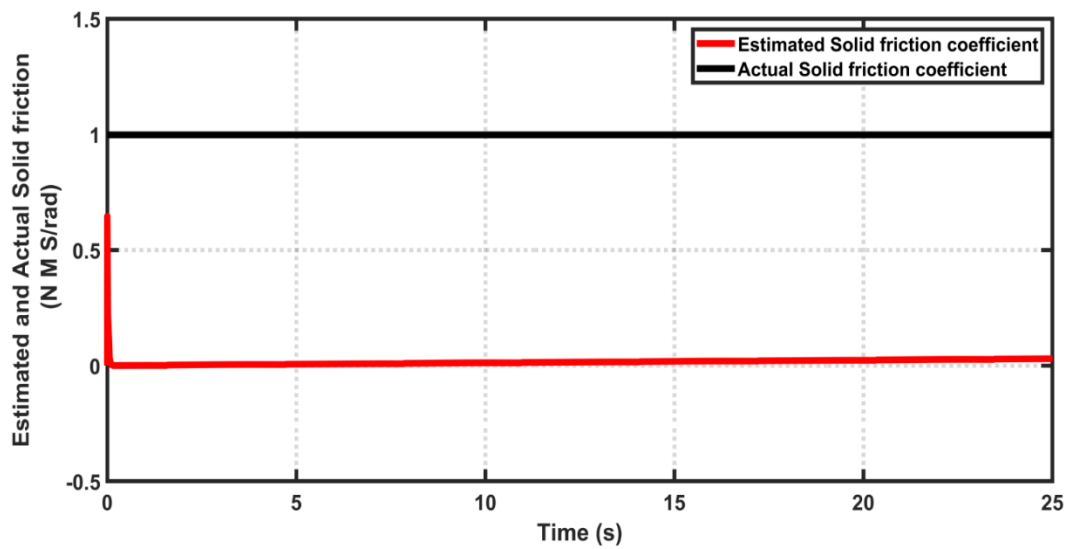


Figure 12. Behaviors of actual and estimated solid friction coefficients f_s .

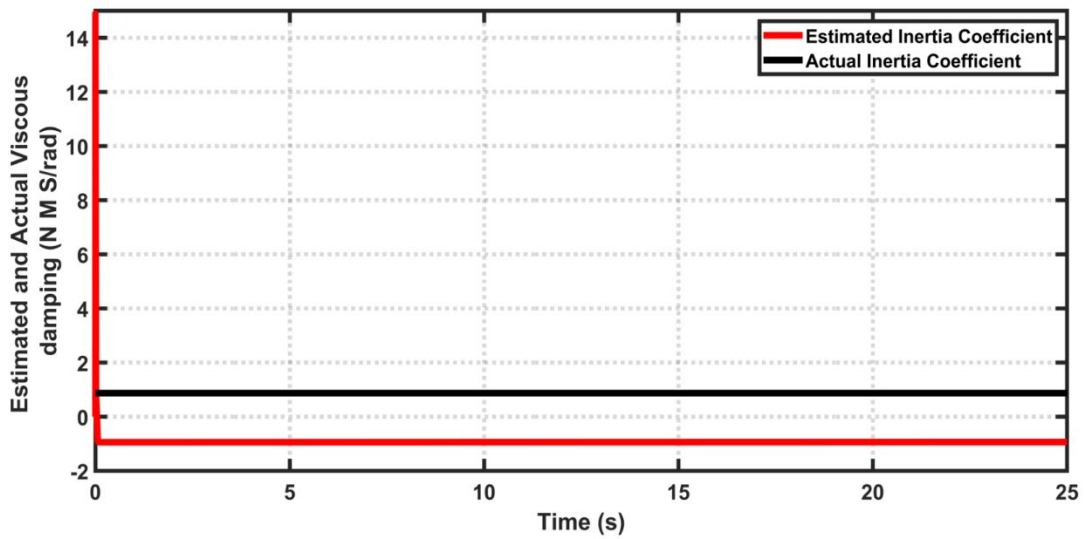


Figure 13. Behaviors of actual and estimated viscous damping coefficients f_v .

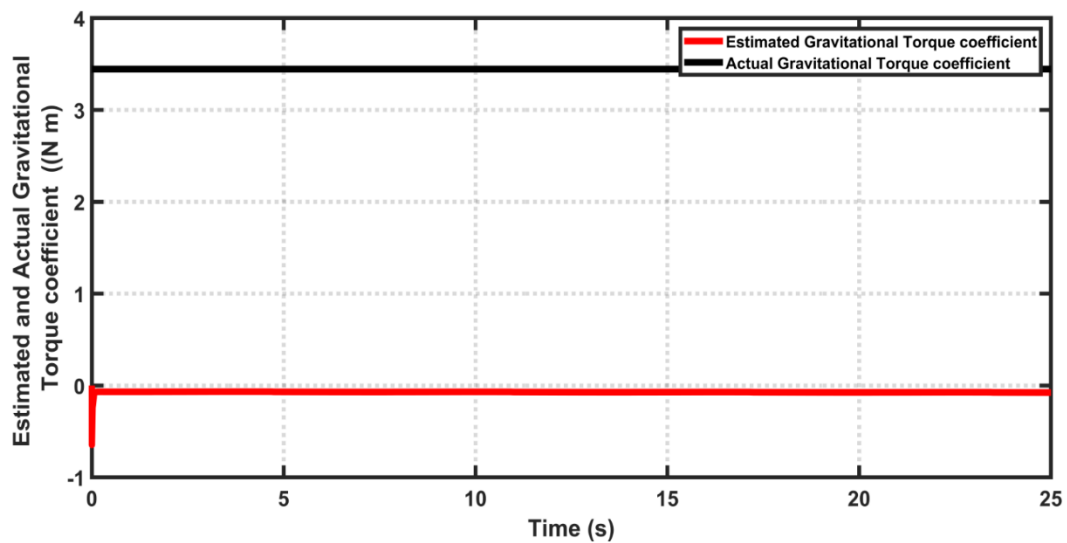


Figure 14. Behaviors of actual and estimated gravitational torque coefficients τ_g .

5. Discussion

According to Figures 3 and 4, it is clear that the cost function decreases with the number of iterations of the PSO algorithm. This indicates that there is an improvement in the dynamic performances of both control schemes. At the end of the iterations, the optimal performances of the controllers can be reached. At this point, the errors in the cost functions are at their minimum values. Based on Figure 6, the PSO algorithm resulted in an 8% improvement in the dynamic performance of the joint angle based on CSC, compared to the trial-and-error procedure. On the other hand, the optimizer resulted in a 5% improvement for the velocity dynamic of the knee joint, compared to the non-optimal case. In the case of ASC, the optimal tuner resulted in a 5% improvement in joint angle performance compared to the conventional trial-and-error procedure, as indicated in Figure 9. However, according to Figure 11, it is evident that the required torque for achieving the optimal performance is higher than that based on the trial-and-error procedure. This is the price to be paid for improvement. The main feature of ASC is that it could guarantee the stability of the controlled system in the presence of uncertainties. According to Equations (32)–(34), the adaptive synergetic controller estimates these uncertainties in f_v , f_s , and τ_g so that the stability is ensured, and no drift occurs in these estimates. According to Figures 12–14, the estimation errors for the estimation parameters are bounded, and this boundedness could prevent the instability problems that might occur in the dynamic response of the knee-joint angle.

6. Conclusions

This study addressed the control design for an assistive system for knee rehabilitation based on a synergetic control methodology. Firstly, the control law was derived based on classical synergetic control. Then, the adaptive synergetic control laws were developed, taking into account the uncertainties in system coefficients based on a Lyapunov-based stability analysis. The adaptive laws are responsible for estimating the uncertainties in coefficients such that stability is ensured and guaranteed. The PSO algorithm was applied to tune the design parameters of both adaptive and non-adaptive synergetic controllers, to further enhance the controlled system. The computer simulation verified the effectiveness of the proposed controllers and the optimizer. The results showed that the adaptive controller could successfully cope with uncertainties in the system parameters, keep the estimated coefficients bounded, and avoid their drifting. In addition, the PSO tuner could improve the dynamic performances of the proposed controllers.

This study could be extended in future work by conducting a comparison study between the proposed PSO algorithm and other optimization techniques such as the cuckoo optimization algorithm, social spider optimization, spider monkey optimization, the whale optimization algorithm, grey wolf optimization, the sine cosine algorithm, and the entropy method [37–45]. Another extension of this study could be to implement the proposed controller in a real-time environment, either using LabVIEW programming software or using other embedded hardware designs such as FPGA or Raspberry Pi [46]. Other control techniques could be suggested to conduct a comparison study for this medical application [47–50].

Author Contributions: Conceptualization, A.J.H., S.M.M., N.Q.Y.; Data curation, S.M.M., N.Q.Y., A.A.O., M.E.S., A.T.A.; Formal analysis, S.M.M., N.Q.Y., A.A.O., M.E.S., A.T.A., A.J.H.; Investigation, A.T.A., M.E.S., A.J.H.; Methodology, S.M.M., N.Q.Y., A.A.O., M.E.S., A.T.A., A.J.H.; Resources, S.M.M., N.Q.Y., A.A.O., M.E.S., A.T.A., A.J.H.; Software, S.M.M., N.Q.Y., A.A.O., M.E.S.; Supervision, A.J.H. and A.T.A.; Validation, A.A.O., A.T.A.; Visualization, S.M.M., N.Q.Y., A.A.O., M.E.S., A.T.A., A.J.H.; Writing—original draft S.M.M., N.Q.Y., A.A.O., M.E.S., A.J.H.; Writing—review & editing, S.M.M., N.Q.Y., A.A.O., M.E.S., A.T.A., A.J.H. All authors have read and agreed to the published version of the manuscript.

Funding: This research received no external funding.

Institutional Review Board Statement: Not applicable.

Informed Consent Statement: Not applicable.

Data Availability Statement: Not applicable.

Acknowledgments: The authors would like to acknowledge the support of Prince Sultan University and the University of Technology-Iraq for supporting this publication. Special acknowledgement is given to the Automated Systems & Soft Computing Lab (ASSCL), Prince Sultan University, Riyadh, Saudi Arabia. In addition, the authors wish to acknowledge the editor and anonymous reviewers for their insightful comments, which have improved the quality of this publication.

Conflicts of Interest: The authors declare no conflict of interest.

References

1. Nasser, A.R.; Hasan, A.M.; Humaidi, A.J.; Alkhayyat, A.; Alzubaidi, L.; Fadhel, M.A.; Santamaría, J.; Duan, Y. IoT and Cloud Computing in Health-Care: A New Wearable Device and Cloud-Based Deep Learning Algorithm for Monitoring of Diabetes. *Electronics* **2021**, *10*, 2719. [[CrossRef](#)]
2. Ergin, M.A.; Patoglu, V. A self-adjusting knee exoskeleton for robot assisted treatment of knee injuries. In Proceedings of the 2011 IEEE/RSJ International Conference on Intelligent Robots and Systems, San Francisco, CA, USA, 25–30 September 2011; pp. 4917–4922.
3. Veerbeek, J.M.; Langbroek-Amersfoort, A.C.; Van Wegen, E.E.; Meskers, C.G.; Kwakkel, G. Effects of Robot-Assisted Therapy for the Upper Limb After Stroke. *Neurorehabil. Neural Repair.* **2017**, *31*, 107–121. [[CrossRef](#)] [[PubMed](#)]
4. Rifai, H.; Mohammed, S.; Daachi, B.; Amirat, Y. Adaptive control of a human-driven knee joint orthosis. In Proceedings of the IEEE International Conference on Robotics and Automation, Saint Paul, MN, USA, 14–18 May 2012; pp. 2486–2491.
5. Sherwani, K.I.K.; Kumar, N.; Chemori, A.; Khan, M.; Mohammed, S. RISE-based adaptive control for EICoSI exoskeleton to assist knee joint mobility. *Robot. Auton. Syst.* **2019**, *124*, 103354. [[CrossRef](#)]
6. Raheema, M.N.; Kadhim, D.A.; Hussein, J.S. Design an intelligent hybrid position/force control for above knee prosthesis based on adaptive neuro-fuzzy inference system. *Indones. J. Electr. Eng. Comput. Sci.* **2021**, *23*, 675–685. [[CrossRef](#)]
7. Ding, G.; Huo, W.; Huang, J.; Amirat, Y.; Mohammed, S. Robust and Safe Control of a Knee Joint Orthosis. In Proceedings of the IEEE International Conference on Intelligence and Safety for Robotics (ISR), Shenyang, China, 24–27 August 2018; pp. 343–348.
8. Mefoued, S.; Mohammed, S.; Amirat, Y. Knee joint movement assistance through robust control of an actuated orthosis. In Proceedings of the IEEE/RSJ International Conference on Intelligent Robots and Systems, San Francisco, CA, USA, 25–30 September 2011; pp. 1749–1754.
9. Zhao, W.; Song, A. Active motion control of a knee exoskeleton driven by antagonistic pneumatic muscle actuators. *Actuators* **2020**, *9*, 134. [[CrossRef](#)]
10. Ajayi, M.O.; Djouani, K.; Hamam, Y. Bounded Control of an Actuated Lower-Limb Exoskeleton. *J. Robot.* **2017**, *2017*, 2423643. [[CrossRef](#)]
11. Aguilar-Sierra, H.; Yu, W.; Salazar, S.; Lopez, R. Design and control of hybrid actuation lower limb exoskeleton. *Adv. Mech. Eng.* **2015**, *7*, 1687814015590988. [[CrossRef](#)]
12. Lee, T.; Lee, D.; Song, B.; Baek, Y.S. Design and Control of a Polycentric Knee Exoskeleton Using an Electro-Hydraulic Actuator. *Sensors* **2020**, *20*, 211. [[CrossRef](#)]
13. Rifai, H.; Ben Abdesslem, M.S.; Chemori, A.; Mohammed, S.; Amirat, Y. Augmented L1 adaptive control of an actuated knee joint exoskeleton: From design to real-time experiments. In Proceedings of the IEEE International Conference on Robotics and Automation (ICRA), Stockholm, Sweden, 16–21 May 2016; pp. 5708–5714.
14. Mefoued, S.; Belkhiat, D.E.C. A Robust Control Scheme Based on Sliding Mode Observer to Drive a Knee-Exoskeleton. *Asian J. Control* **2019**, *21*, 439–455. [[CrossRef](#)]
15. Chen, C.; Du, Z.; He, L.; Wang, J.; Wu, D.; Dong, W. Active Disturbance Rejection with Fast Terminal Sliding Mode Control for a Lower Limb Exoskeleton in Swing Phase. *IEEE Access* **2019**, *7*, 72343–72357. [[CrossRef](#)]
16. Wang, J.; Liu, J.; Chen, L.; Guo, S. Observer-based finite-time control for trajectory tracking of lower extremity exoskeleton. *Proc. Inst. Mech. Eng. Part I J. Syst. Control Eng.* **2021**, *236*, 257–269. [[CrossRef](#)]
17. Chevalier, A.; Ionescu, C.M.; Keyser, R.D. Analysis of robustness to gain variation in a fractional-order PI controller for knee joint motion. In Proceedings of the ICFDA'14 International Conference on Fractional Differentiation and Its Applications 2014, Catania, Italy, 23–25 June 2014; pp. 1–6.
18. Kaur, S.; Sagar, S.; Sondhi, S. Internal model control based fractional order PID controller for knee joint motion. In Proceedings of the 11th International Conference on Industrial and Information Systems (ICIIS), Roorkee, India, 3–4 December 2016; pp. 318–322.
19. Mefoued, S.; Mohammed, S.; Amirat, Y. Toward Movement Restoration of Knee Joint Using Robust Control of Powered Orthosis. *IEEE Trans. Control Syst. Technol.* **2013**, *21*, 2156–2168. [[CrossRef](#)]
20. Mefoued, S. A robust adaptive neural control scheme to drive an actuated orthosis for assistance of knee movements. *Neurocomputing* **2014**, *140*, 27–40. [[CrossRef](#)]
21. Wang, T.K.; Ju, M.S.; Tsuei, Y.G. Adaptive Control of Above Knee Electro-Hydraulic Prosthesis. *J. Biomech. Eng.* **1992**, *114*, 421–424. [[CrossRef](#)]

22. Zhang, Y.; Wang, J.; Li, W.; Wang, J.; Yang, P. Model-free control method for estimating the joint angles of the knee exoskeleton. *Adv. Mech. Eng.* **2018**, *10*, 1687814018807768. [[CrossRef](#)]
23. Guan, W.; Zhou, L.; Cao, Y. Joint Motion Control for Lower Limb Rehabilitation Based on Iterative Learning Control (ILC) Algorithm. *Complexity* **2021**, *2021*, 1–9. [[CrossRef](#)]
24. Aljuboury, A.S.; Hameed, A.H.; Ajel, A.R.; Humaidi, A.J.; Alkhayyat, A.; Mhdawi, A.K.A. Robust adaptive control of knee exoskeleton-assistant system based on nonlinear disturbance observer. *Actuators* **2022**, *11*, 78. [[CrossRef](#)]
25. Aole, S.; Elamvazuthi, I.; Waghmare, L.; Patre, B.; Meriaudeau, F. Improved active disturbance rejection control for trajectory tracking control of lower limb robotic rehabilitation exoskeleton. *Sensors* **2020**, *20*, 3681. [[CrossRef](#)]
26. Zhan, L.; Wenhao, M.; Ziguang, Y.; Hongliang, G. Tracking control of time-varying knee exoskeleton disturbed by interaction torque. *ISA Trans.* **2017**, *71*, 458–466.
27. Shepherd, M.K.; Rouse, E.J. Design and Validation of a Torque-Controllable Knee Exoskeleton for Sit-to-Stand Assistance. *IEEE/ASME Trans. Mechatron.* **2017**, *22*, 1695–1704. [[CrossRef](#)]
28. Lyu, M.; Chen, W.-H.; Ding, X.; Wang, J.; Pei, Z.; Zhang, B. Development of an EMG-Controlled Knee Exoskeleton to Assist Home Rehabilitation in a Game Context. *Front. Neurobot.* **2019**, *13*, 67. [[CrossRef](#)] [[PubMed](#)]
29. Qian, J.; Li, K.; Wu, H.; Yang, J.; Li, X. Synergetic Control of Grid-Connected Photovoltaic Systems. *Int. J. Photoenergy* **2017**, *2017*, 5051489. [[CrossRef](#)]
30. Yang, X.; Jiah, Y. Adaptive Synergetic Control about Attitude Tracking of Rigid Spacecraft with Disturbances and Parameter Uncertainties. In Proceedings of the 15th International Conference on Control, Automation and Systems (ICCAS 2015), Busan, Korea, 13–16 October 2015; pp. 13–16.
31. Humaidi, A.J.; Ibraheem, I.K.; Azar, A.T.; Sadiq, M.E. A New Adaptive Synergetic Control Design for Single Link Robot Arm Actuated by Pneumatic Muscles. *Entropy* **2020**, *22*, 723. [[CrossRef](#)] [[PubMed](#)]
32. Humaidi, A.J.; Hameed, M. Development of a New Adaptive Backstepping Control Design for a Non-Strict and Under-Actuated System Based on a PSO Tuner. *Information* **2019**, *10*, 38. [[CrossRef](#)]
33. Humaidi, A.J.; Kadhim, S.K.; Gata, A. Optimal Adaptive Magnetic Suspension Control of Rotary Impeller for Artificial Heart Pump. *Cybern. Syst.* **2022**, *53*, 141–167. [[CrossRef](#)]
34. Humaidi, A.J.; Badr, H.M. Linear and Nonlinear Active Disturbance Rejection Controllers for Single-Link Flexible Joint Robot Manipulator based on PSO Tuner. *J. Eng. Sci. Technol. Rev.* **2018**, *11*, 133–138. [[CrossRef](#)]
35. Humaidi, A.J.; Kadhim, S.K.; Gataa, A.S. Development of a Novel Optimal Backstepping Control Algorithm of Magnetic Impeller-Bearing System for Artificial Heart Ventricle Pump. *Cybern. Syst.* **2020**, *51*, 521–541. [[CrossRef](#)]
36. Alawad, N.A.; Humaidi, A.J.; Al-Araji, A.S. Improved Active Disturbance Rejection Control for the Knee Joint Motion Model. *Math. Model. Eng. Probl.* **2022**, *9*, 477–483. [[CrossRef](#)]
37. Moezi, S.A.; Zakeri, E.; Zare, A. A generally modified cuckoo optimization algorithm for crack detection in cantilever Euler-Bernoulli beams. *Precis. Eng.* **2018**, *52*, 227–241. [[CrossRef](#)]
38. Tang, R.; Fong, S.; Dey, N.; Wong, R.K.; Mohammed, S. Cross Entropy Method Based Hybridization of Dynamic Group Optimization Algorithm. *Entropy* **2017**, *19*, 533. [[CrossRef](#)]
39. Al-Azza, A.A.; Al-Jodah, A.A.; Harackiewicz, F.J. Spider monkey optimization: A novel technique for antenna optimization. *IEEE Antennas Wirel. Propag. Lett.* **2015**, *15*, 1016–1019. [[CrossRef](#)]
40. Al-Qassar, A.A.; Al-Obaidi, A.S.; Hasan, A.F.; Humaidi, A.J.; Nasser, A.R.; Alkhayyat, A.; Ibraheem, K.I. Finite-Time Control of Wing-Rock Motion for Delta Wing Aircraft Based on Whale-Optimization Algorithm. *Indones. J. Sci. Technol.* **2021**, *6*, 441–456. [[CrossRef](#)]
41. Gao, Z.-M.; Zhao, J. An Improved Grey Wolf Optimization Algorithm with Variable Weights. *Comput. Intell. Neurosci.* **2019**, *2019*, 2981282. [[CrossRef](#)] [[PubMed](#)]
42. Al-Qassar, A.A.; Abdu-Alkareem, A.I.; Hasan, A.F.; Humaidi, A.J.; Ibraheem, K.I.; Azar, A.T.; Hameed, A.H. Grey-Wolf Optimization Better Enhances the Dynamic Performance of Roll Motion for Tail-Sitter VTOL Aircraft Guided and Controlled by STSMC. *J. Eng. Sci. Technol.* **2021**, *16*, 1932–1950.
43. Humaidi, A.J.; Najem, H.T.; Al-Dujaili, A.Q.; Pereira, D.A.; Ibraheem, I.K.; Azar, A.T. Social spider optimization algorithm for tuning parameters in PD-like interval type-2 fuzzy logic controller applied to a parallel robot. *Meas. Control* **2021**, *54*, 303–323. [[CrossRef](#)]
44. Nasiri, J.; Khiyabani, F.M. A whale optimization algorithm (WOA) approach for clustering. *Cogent Math. Stat.* **2018**, *5*, 1483565. [[CrossRef](#)]
45. Mirjalili, S. A Sine Cosine Algorithm for solving optimization problems. *Knowl. Based Syst.* **2016**, *96*, 120–133. [[CrossRef](#)]
46. Kasim, M.Q.; Hassan, R.F.; Humaidi, A.J.; Abdulkareem, A.I.; Nasser, A.R.; Alkhayyat, A. Control Algorithm of Five-Level Asymmetric Stacked Converter Based on Xilinx System Generator. In Proceedings of the IEEE 9th Conference on Systems, Process and Control (ICSPC 2021), Malacca, Malaysia, 10–11 December 2021; pp. 174–179.
47. Hameed, A.H.; Al-Dujaili, A.Q.; Humaidi, A.J.; Hussein, H.A. Design of terminal sliding position control for electronic throttle valve system: A performance comparative study. *Int. Rev. Autom. Control* **2019**, *12*, 251–260. [[CrossRef](#)]
48. Humaidi, A.J.; Hameed, A.H. Design and comparative study of advanced adaptive control schemes for position control of electronic throttle valve. *Information* **2019**, *10*, 65. [[CrossRef](#)]

49. Humaidi, A.J.; Hameed, M.R. Design and performance investigation of block-backstepping algorithms for ball and arc system. In Proceedings of the 2017 IEEE International Conference on Power, Control, Signals and Instrumentation Engineering (ICPSI), Chennai, India, 21–22 September 2017; pp. 325–332.
50. Berbek, M.I.; Oglah, A.A. Adaptive neuro-fuzzy controller trained by genetic-particle swarm for active queue management in internet congestion. *Indones. J. Electr. Eng. Comput. Sci.* **2022**, *26*, 229–242. [[CrossRef](#)]